

# Dynamics of Ordering of Isotropic Magnets

Jayajit Das<sup>†</sup>

*Institute of Mathematical Sciences, CIT Campus, Taramani, Madras 600113, India*

and

Madan Rao<sup>\*</sup>

*Raman Research Institute, C.V. Raman Avenue, Sadashivanagar, Bangalore 560080, India*  
(April 24, 2017)

We study the dynamics of ordering of the nonconserved and conserved Heisenberg magnet. The dynamics consists of two parts – an irreversible dissipation into a heat bath and a reversible precession induced by a torque due to the local molecular field. For quenches both to  $T = 0$  and  $T = T_c$ , we show that the torque is irrelevant when the dynamics is nonconserved but relevant when the dynamics is conserved and is governed by a new nontrivial fixed point.

64.60.My, 64.60.Cn, 68.35.Fx, 81.30.Kf

Keywords : Heisenberg magnet, Langevin equation, Dynamical scaling, Multiscaling.

## I. INTRODUCTION

Most interacting systems like magnets and binary fluids when quenched from the disordered phase to zero temperature, evolve extremely slowly to establish order, primarily because of the slow annealing of the interfaces (defects) separating the competing domains. It is seen that at late times, the system organizes itself into a self similar spatial distribution of domains characterised by a single diverging length scale which typically grows algebraically in time  $L(t) \sim t^{1/z}$ . The equal-time order parameter correlation function  $C(r, t) \equiv \langle \vec{\phi}(r, t) \cdot \vec{\phi}(0, t) \rangle$  is a measure of the spatial distribution of the domains, and at late times is found to behave as  $f(r/L(t))$ , where  $L(t)$  is the distance between defects. The autocorrelation function,  $C(0, t_1 = 0, t_2) \equiv \langle \vec{\phi}(0, 0) \cdot \vec{\phi}(0, t_2) \rangle$ , is a measure of the memory of the initial configurations, and decays at late times as  $L(t_2)^{-\lambda}$ . The independent scaling exponents  $z$  and  $\lambda$  and the scaling function  $f(x)$  characterise the dynamical universality classes at the zero temperature fixed point [1].

There has been a trend in recent years to compare the theories of phase ordering dynamics with numerical simulations of Langevin equations. Comparison with experimental systems, such as magnets, binary fluids or binary alloys have to take into account the various ‘real’ features that might be relevant to its late time dynamics. For instance, theories of binary fluids have to include effects of hydrodynamics, while those of binary alloys have to incorporate elastic and hydrodynamic effects. In the same vein, any comparison with the dynamics in real magnets has to include the effects of the torque induced by the local molecular field [2,3].

## II. PHASE ORDERING DYNAMICS : QUENCHES TO $T = 0$

The spins  $\phi_\alpha$  ( $\alpha = 1, 2, 3$ ) in a Heisenberg ferromagnet in three dimensions experience a torque from the joint action of the external field (if present) and the local molecular field. In response the spins precess with a Larmour frequency  $\Omega_L$  about the total magnetic field. Coupling to various faster degrees of freedom like phonons, electrons and magnons causes dissipation and an eventual relaxation towards equilibrium.

The equations of motion in dimensionless variables is given by [2],

$$\frac{\partial \vec{\phi}}{\partial t} = -(-i\nabla)^\mu \left( \nabla^2 \vec{\phi} + \vec{\phi} - (\vec{\phi} \cdot \vec{\phi}) \vec{\phi} \right) + g \left( \vec{\phi} \times \nabla^2 \vec{\phi} \right). \quad (1)$$

The exponent  $\mu$  in the above equation takes the value 0 when the magnetisation is not conserved (NCOP) and 2 when it is conserved (COP). The dimensionless parameter  $g \sim \Omega_L/\Gamma$  is the ratio of the precession frequency to the relaxation rate, which is in the range  $g \sim 10^{-3} - 10$  for typical ferromagnets.

## A. Langevin Simulation

We prepare the system in the paramagnetic phase and quench to zero temperature. We study the time evolution of the spin configurations as they evolve according to Eq. (1). We calculate the spatially averaged equal time correlator  $C(\mathbf{r}, t)$  and the autocorrelator  $C(\mathbf{0}, t_0 = 0, t)$ , both averaged over the random initial conditions. We compute the scaling exponents  $z$  and  $\lambda$  and the scaling function  $f(r/L(t))$  as defined above.  $L(t)$ , a measure of the distance between defects, is extracted both from  $C(\mathbf{r}, t)$  and from the scaling form of the energy density,  $\varepsilon = \frac{1}{V} \int d\mathbf{r} \langle (\nabla \phi(\mathbf{r}, t))^2 \rangle$ .

We discretize Eq. (1) on a simple cubic lattice of size  $N$  ranging from  $40^3$  to  $60^3$ , adopting an Euler scheme for the derivatives [10] with periodic boundary conditions. The space and time intervals have been chosen to be  $\Delta x = 3$ ,  $\Delta t = 0.01$  (NCOP) and  $\Delta x = 2.5$ ,  $\Delta t = 0.20$  (COP). Further details of the simulation may be found in [2,3].

### 1. Non-Conserved Case

We will show that the torque is irrelevant in  $d = 3$ , which means that the asymptotic values of  $z$ ,  $\lambda$  and the scaling form  $f(x)$  remain unchanged and independent of  $g$ . The correlation functions have been computed for  $g$  ranging from 0 to 5. The dynamical exponent is found to be unchanged from  $z = 2$  (within statistical errors) and independent of  $g$  [2]. Likewise the autocorrelation exponent is unchanged from its  $g = 0$  value and equal to  $\lambda \approx 1.52$  independent of  $g$ . Note that the numerical determination of  $\lambda$  is subject to large errors [2,4], and so we have to go to very late times and hence large system sizes.

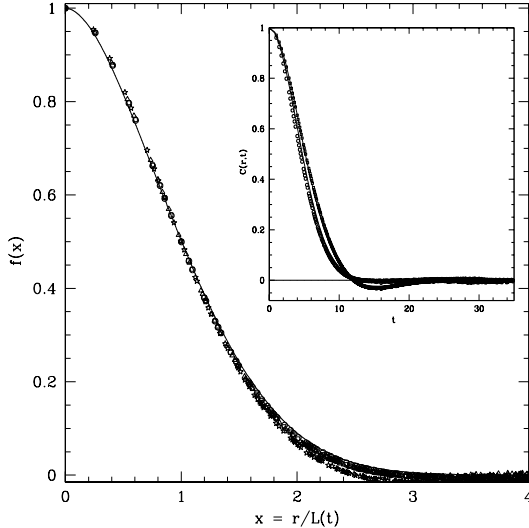


Fig. 1. Scaling plot of  $C(r, t) \equiv f(x)$  versus  $x \equiv r/L(t)$  for  $g = 0(\circ)$ ,  $0.5(\triangle)$ ,  $2(*)$ . The solid line through the data points is a fit to the BPT function [5]. Inset compares  $C(\mathbf{r}, t)$  for  $g = 1(\circ)$  with  $g = 5(\square)$  at late times. The solid line through these data points comes from a preasymptotic analysis (see below) of  $C(r, t)$  [2].

The scaling function  $f(x)$  is also unchanged and independent of  $g$ . This is clearly apparent for  $g = 0, 0.5, 1, 2$  (Fig. 1). However at larger values of  $g$ , the correlation function crosses zero at large  $r$ , dips through a minimum, and then asymptotically goes to zero (of course  $\int C(r, t) > 0$ ). It would appear that  $C(r/L(t))$  for  $g = 5$  is qualitatively different from the scaling function for  $g = 0$ . However we note that the dip decreases very slowly with increasing time suggesting it might disappear at late times. Patience confirms this for intermediate values of  $g$  (between 2 and 5). When  $g = 5$ , finite size effects prevent the system from exploring its true asymptotic regime, when the order parameter field has totally relaxed with respect to defect cores. Pre-asymptotic configurations typically consist of spin wave excitations interspersed between slowly moving defects separated by a distance  $L(t) \gg \xi$ , the size of the defect core. Decomposing  $\vec{\phi}$  into a singular (defect) part  $\vec{\phi}_{sing}$  and a smooth (spin wave) part  $\vec{\phi}_{sm}$  gives the preasymptotic correlation function three contributions –  $C_{sing} \equiv \langle \vec{\phi}_{sing}(0, t) \cdot \vec{\phi}_{sing}(\mathbf{r}, t) \rangle$  (defect contributions),  $C_{sm} \equiv \langle \vec{\phi}_{sm}(0, t) \cdot \vec{\phi}_{sm}(\mathbf{r}, t) \rangle$  (spin wave contributions) and  $C_{scat} \equiv \langle \vec{\phi}_{sm}(0, t) \cdot \vec{\phi}_{sing}(\mathbf{r}, t) \rangle$  (scattering of spin waves off slowly moving defects). The defect

contribution  $C_{sing}$  takes the form given in [5], while the spin wave contribution  $C_{sm}$  can be evaluated perturbatively [2]. Even without including the scattering between spin waves and defects, we find that the total correlation function has a dip when  $g \neq 0$  as shown by the solid line in the inset of Fig. 1. The long lifetime of the dip arises because of the slow relaxation of the spin waves as they scatter off the slow moving defects.

## 2. Conserved Case

When the dynamics is conserved, we show that the the torque  $g$  drives the system to a new fixed point characterised by a different value of  $z$ ,  $\lambda$  and the scaling function  $f(x)$ . Moreover these quantities are independent of the value of  $g$  as long as it is  $g > 0$ . This crossover is described by a crossover exponent and a crossover function.

Figure 2 shows that the scaling function for  $g = 0$  is very different from those for  $g > 0$  and the  $g > 0$  scaling functions do not depend on the value of  $g$ . The  $z$  exponent crosses over from  $z = 4$  (its value at  $g = 0$ ) when  $t < t_c(g)$  to  $z = 2$  when  $t > t_c(g)$  where  $t_c(g)$  is the crossover time which decreases with increasing  $g$  (Fig. 2(inset)). Likewise the autocorrelation exponent  $\lambda$  crosses over from  $\lambda \approx 2.2$  when  $g = 0$  to  $\lambda \approx 5.15$  when  $g > 0$  [3].

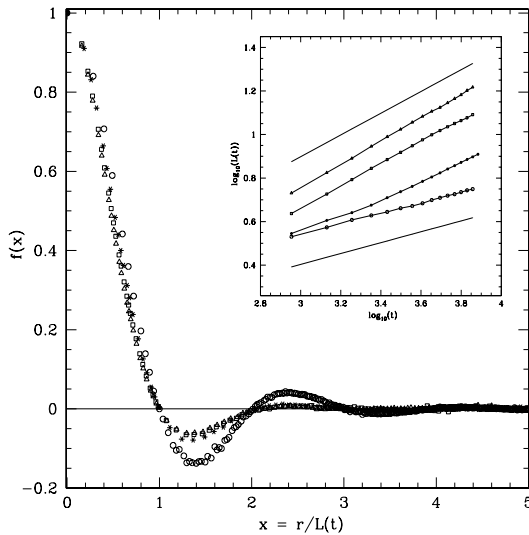


Fig. 2. Scaling plot of  $C(\mathbf{r}, t)$  comparing  $g = 0$  ( $\circ$ ) with  $g > 0$  ( $g = 0.1$  (\*),  $0.3$  ( $\triangle$ )),  $0.5$  ( $\square$ )). Inset shows log-log plot of  $L(t)$  versus  $t$ . At  $g = 0$  ( $\circ$ ),  $z = 4$  (line of slope 0.25 drawn for comparison). At other values of  $g$  ( $g = 0.1$  (\*),  $0.3$  ( $\square$ ),  $0.5$  ( $\triangle$ )),  $z$  crosses over from 4 to 2 (line of slope 0.5 drawn for comparison).

The crossover may be understood from a simple scaling argument [3]. On restoring appropriate dimensions, the dynamical equation Eq.(1) can be rewritten as a continuity equation,  $\partial \vec{\phi}(\mathbf{r}, t)/\partial t = -\nabla \cdot \vec{j}$  where the ‘spin current’

$$\vec{j}_\alpha = -\Gamma \left( \nabla \frac{\delta F[\vec{\phi}]}{\delta \phi_\alpha} + \frac{\Omega}{\Gamma} \epsilon_{\alpha\beta\gamma} \phi_\beta \nabla \phi_\gamma \right). \quad (2)$$

Using a dimensional analysis where we replace  $j_\alpha$  by the ‘velocity’  $dL/dt$ , we find

$$\frac{dL}{dt} = \Gamma \frac{\sigma}{L^3} + \Omega \frac{\sigma M_0}{L}, \quad (3)$$

where the parameters  $M_0$ ,  $\sigma$  and  $\Gamma^{-1}$  are the equilibrium magnetisation, surface tension and spin mobility respectively. Beyond a crossover time  $t_c(g) \sim (\Gamma/M_0\Omega)^2 \sim 1/g^2$ , simple dimension counting shows that the dynamics crosses over from  $z = 4$  to  $z = 2$  in conformity with our numerical simulation. Our numerics supports a scaling form  $L(t, g) = t^{1/4} s(tg^\phi)$  with  $\phi \approx 1.7$ , valid for all  $g$  [3].

## B. Numerical Tests of the Mazenko Closure Scheme

There is a class of approximate theories based on the gaussian closure approximation [6,1] that is supposed to provide fairly successful predictions for the forms of the correlation functions. We will show that the gaussian closure approximation works fairly well for the nonconserved Heisenberg model with  $g \geq 0$  and leads to conclusions similar to the ones described in the previous section. In contrast, the use of the gaussian closure in conserved models leads to sharp inconsistencies.

The gaussian closure method consists of trading the order parameter  $\vec{\phi}(\mathbf{r}, t)$  which is singular at defect sites, for an everywhere smooth field  $\vec{m}(\mathbf{r}, t)$ , defined by a nonlinear transformation,  $\vec{\phi}(\mathbf{r}, t) = \vec{\sigma}(\vec{m}(\mathbf{r}, t))$ . An appropriate choice for this nonlinear function  $\vec{\sigma}$  is an equilibrium defect profile,

$$\vec{\sigma}(\vec{m}(\mathbf{r}, t)) = \frac{\vec{m}(\mathbf{r}, t)}{|\vec{m}(\mathbf{r}, t)|} g(|\vec{m}|), \quad (4)$$

where  $g(0) = 0$  and  $g(\infty) = 1$ . With this choice,  $|\vec{m}|$  has the interpretation of being the distance away from a defect core. Correlation functions are calculated making the single assumption that each component of  $\vec{m}(\mathbf{r}, t)$  is an independent gaussian field with zero mean at all times [6,1].

To check whether this is a good approximation we compute  $\vec{\phi}$  numerically and then determine  $\vec{m}(\mathbf{r}, t)$  by inverting Eq. (4). We then calculate both the single point probability distribution  $P(\vec{m}(\mathbf{r}, t))$  and the joint probability distribution in the scaling regime and compare with the gaussian assumption of Mazenko. These computations require a lot of averaging over initial configurations to obtain good statistics.

### 1. Nonconserved Case

Figure 3 shows the scaling plots of  $P(m_1(\mathbf{r}, t))$  ( $m_1$  is a component of  $\vec{m}$ ) at  $g = 0$  and  $g = 1$ . Since  $m$  has dimensions of length, the appropriate scaling variable is  $m_1/L(t)$  [2]. The scaled distribution  $P(m_1)$  is seen to be the same for  $g = 0$  and  $g = 1$ , suggesting that it is unchanged on addition of the torque. We also find that it is independent of  $g$ .

The scaled distribution  $P(m_1)$  closely resembles a gaussian at late times (this is confirmed by a more detailed analysis [2]). The calculated joint probability distribution also agrees reasonably well with the Mazenko assumption [2]. These findings are consistent with a similar analysis done on a scalar order parameter [7].

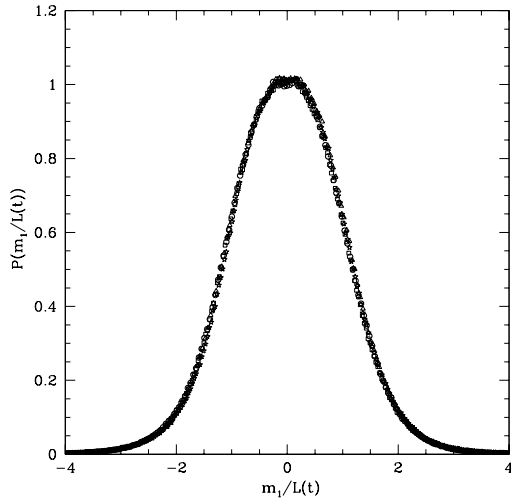


Fig. 3. Scaling plot of the un-normalised  $P(m_1)$  for  $g = 0$  ( $t = 5000(\circ)$ ,  $t = 10000(\square)$ ) and  $g = 1$  ( $t = 5000(\triangle)$ ,  $t = 10000(*)$ ).

## 2. Conserved Case

In the conserved case, the single point probability density  $P(m_1(\mathbf{r}, t))$  scales at late times, but the scaled distribution is distinctly flatter than a gaussian (Fig. 4). Apart from this strong deviation we find that the gaussian assumption leads to an internal inconsistency, using a criterion initially developed by Yeung et. al. [7] for a conserved scalar order parameter.

We numerically evaluate the spectral density, the fourier transform of  $\gamma(r, t) = \langle \vec{m}(\mathbf{r} + \mathbf{x}, t) \cdot \vec{m}(\mathbf{x}, t) \rangle / \langle m^2(\mathbf{r}, t) \rangle$ . We observe [3] that the spectral density, which should be a strictly positive function of its arguments, becomes negative for  $k/k_m < 0.5$  ( $\gamma(k, t)$  is peaked at  $k_m$ ) and in the range  $1.5 < k/k_m < 3.0$  ! This demonstration highlights the intrinsic inconsistency of the gaussian approach for conserved vector order parameters.

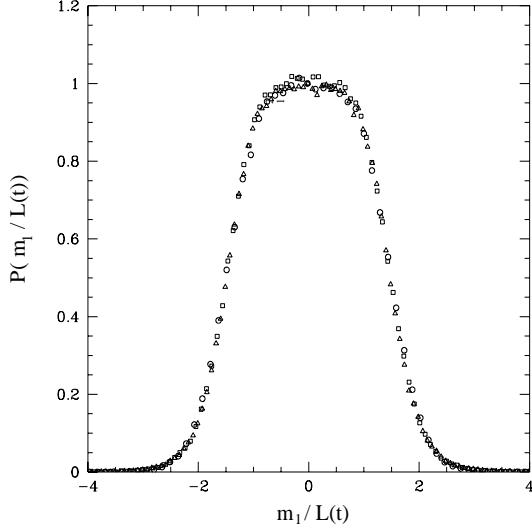


Fig. 4. Scaling plot of the un-normalised  $P(m_1)$  for  $g = 0$  at different times  $t = 900(\circ)$ ,  $t = 3600(\square)$ ,  $t = 6300(\triangle)$ .

## C. Multiscaling Analysis

We have just seen that the Mazenko assumption of a gaussian probability distribution fails sharply when the dynamics conserves the total magnetisation. This seems to lead to an interesting technical problem. Coniglio and Zannetti [8] had explicitly shown that the late time dynamics of a conserved  $n$ -component spin model in the limit  $n \rightarrow \infty$  reveals an infinity of length scales leading to a more complicated multiscaling form for the structure factor (fourier transform of  $C(\mathbf{r}, t)$ )  $S(k, t) \sim L(t)^{p(k/k_m)d}$ . The length scale  $L(t) \sim t^{1/4}$  and the position of the maximum of the structure factor  $k_m^{-1} \sim (t/\ln t)^{1/4}$ , and the scale dependent exponent  $p(x) = 1 - (1 - x^2)^2$ . They went on to speculate that this multiscaling behaviour might be a generic feature of conserved order parameters [8].

Subsequent numerical work showed that for the scalar ( $n = 1$ ) [9], the XY ( $n = 2$ ) [10,11] and  $n = 3, 4$  [11] models, the structure factor obeyed the conventional ‘single length’ scaling form. This suggested the possibility that multiscaling was nongeneric and an ‘aberration’ of the  $n \rightarrow \infty$  model, though there was no general proof.

Bray and Humayun (BH) [12] provided such a ‘proof’. Their analysis was built on the validity of the Mazenko gaussian assumption for all values of  $n$ . Performing a  $1/n$  expansion within the Mazenko framework, they showed that the asymptotic  $S(\mathbf{k}, t)$  exhibited multiscaling only when  $n = \infty$ .

Having just demonstrated that the Mazenko gaussian assumption is inconsistent for the conserved Heisenberg model ( $n = 3$ ), how do we understand the BH proof [12] ? Are the conclusions arrived by BH incorrect ?

We now show that the structure factor  $S(\mathbf{k}, t)$  of the conserved  $n = 3$  model does NOT obey multiscaling, consistent with the main conclusion of BH. This is done using the method described in [10].

The method [10] demands a very accurate determination of  $S(\mathbf{k}, t)$ . Since the numerical evaluation of  $S(\mathbf{k}, t)$  is subject to large errors (especially at small  $k$ ), we fit a function  $C_f(\mathbf{r}, t)$  to the computed  $C(\mathbf{r}, t)$  and then calculate the fourier transform  $S_f(\mathbf{k}, t)$ . The fitting function for  $C_f(\mathbf{r}, t)$  has been taken as  $\sin(r/L)/(r/L)(1 + a(r/L)^2) \exp(-b(r/L)^2)$  which is similar to the analytic form given in [13]. Note that only  $b$  and  $L$  are independent

fitting parameters,  $a$  is determined by the condition  $S_f(k=0, t) = 0$ . We now plot  $S_f(k, t)$  versus  $t$  at fixed values of  $x = k/k_m$  (Fig. 5). The resulting straight lines labeled by different values of  $x$ , all show a constant slope of approximately  $3/4$  (Fig. 5). Using the proposed multiscaling form, a plot of  $p(x)$  versus  $x$  (inset Fig. 5) shows that  $p(x)$  is clustered around 1. The small spread of  $p(x)$  around 1 indicates that we have not quite reached the asymptotic regime, and it is likely that the late time  $p(x) \rightarrow 1$ , in agreement with conventional scaling. In addition, note that the form of  $p(x)$  is qualitatively different from the downward curving  $p(x)$  predicted by Coniglio and Zannetti [8]. We conclude then that the correlation function  $C(\mathbf{r}, t)$  for the  $n = 3$  conserved model does not obey multiscaling.

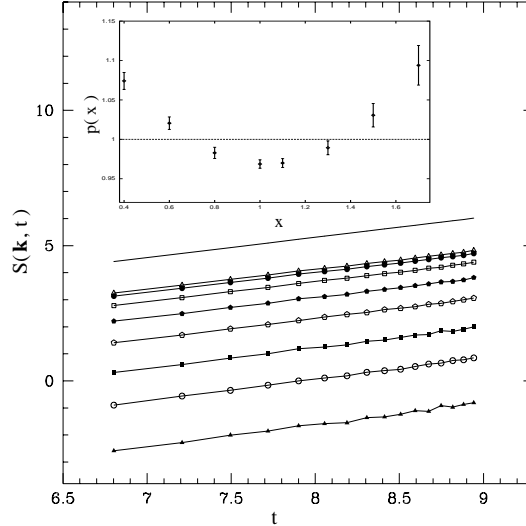


Fig. 5. Plot of  $S(\mathbf{k}, t)$  vs  $t$  for  $x = 0.4$ (circle),  $x = 0.6$ (pentagon),  $x = 0.8$ (square),  $x = 1.0$ (triangle),  $x = 1.1$ (filled circle),  $x = 1.3$ (filled pentagon),  $x = 1.5$ (filled square),  $x = 1.7$ (filled triangle). A straight line of slope  $3/4$  is given for comparison. Inset figure shows plot of  $p(x)$  with  $x$ . Note that the errors in  $p(x)$  increases as  $|x - 1|$  increases because of the smallness of  $S(\mathbf{k}, t)$  near its wings.

Thus we are forced to conclude that since the Mazenko assumption is invalid for conserved vector order parameters (except when  $n = \infty$ ), an analytical proof of the absence of multiscaling of the asymptotic structure factor is still lacking.

### III. PHASE ORDERING DYNAMICS: QUENCHES TO $T = T_C$

We have also studied the asymptotic dynamics following a quench to the critical point [3]. We ask for whether the torque  $g$  is relevant at the Wilson-Fisher fixed point of the pure  $g = 0$  Heisenberg model, both when the magnetisation is conserved and nonconserved.

Power counting reveals that  $g$  is irrelevant for  $d > 2$  when the order parameter is nonconserved. Thus the values of  $z$  and  $\lambda$  are unchanged from the Wilson-Fisher value. For the conserved model, on the other hand, power counting shows that  $g$  is relevant for  $d < 6$ , giving rise to a new fixed point. The dynamical exponent  $z$  changes from the WF value of  $4 - \eta$  to  $z = 4 - \varepsilon/2 + \mathcal{O}(\varepsilon^2)$ , where  $\varepsilon = 4 - d$  and  $\varepsilon = 6 - d$  [14]. The value of the autocorrelation exponent  $\lambda$  is however solely determined by the conservation law; it is always fixed at the spatial dimension  $d$ . This is confirmed by a perturbative analysis to all orders in  $\varepsilon$  [3].

<sup>†</sup> email: jayajit@rri.ernet.in

<sup>\*</sup> email: madan@rri.ernet.in

On leave of absence from: Institute of Mathematical Sciences, CIT Campus, Taramani, Chennai 600 113, India.

[1] A. J. Bray, Adv. Phys. **43** (1994) 357.

- [2] J. Das and M. Rao, Phys. Rev. E **57** (1998) 5069.
- [3] J. Das and M. Rao, IMA Preprint - 99/01/04.
- [4] C. Yeung, M. Rao, and R. C. Desai, Phys. Rev. E **53** (1996) 1.
- [5] The computed  $C(r, t)$  compares well with an approximate form (A. J. Bray and S. Puri, Phys. Rev. Lett. **67** (1991) 2670; H. Toyoki, Phys. Rev. B **45** (1992) 1965.) given by  $f(x) = (3\gamma/2\pi)[B(2, 1/2)]^2 {}_2F_1(1/2, 1/2, 5/2; \gamma^2)$  where  $\gamma = \exp(-x^2/8)$  and  $B$  and  ${}_2F_1$  are the Beta and the hypergeometric functions respectively.
- [6] G. F. Mazenko, Phys. Rev. B **43** (1994) 357; A. J. Bray and K. Humayun, J. Phys. A **25**, (1992) 2191.
- [7] C. Yeung, A. Shinozaki and Y. Oono, Phys. Rev. E **49** (1994) 2693.
- [8] A. Coniglio and M. Zannetti, Europhys. Lett. **10** (1989) 57.
- [9] A. Coniglio, Y. Oono, A. Shinozaki, and M. Zannetti, Europhys. Lett. **18** (1992) 59.
- [10] M. Seigert and M. Rao, Phys. Rev. Lett. **70** (1993) 1956.
- [11] M. Rao, and A. Chakrabarti, Phys. Rev. E **49** (1994) 3727.
- [12] A. J. Bray and K. Humayun, Phys. Rev. Lett. **68** (1992) 1559.
- [13] F. R. Iniguez and A. J. Bray, Phys. Rev. E **51** (1995) 188.
- [14] P. C. Hohenberg and B. I. Halperin, Rev. Mod. Phys. **49** (1977) 436 ; S. K. Ma and G. F. Mazenko, Phys. Rev. B **11** (1975) 4077.